applied sciences

MDPI

Article

# A Large-Diameter Earth–Air Heat Exchanger (EAHX) Built for Standalone Office Room Cooling: Monitoring Results for Hot and Dry Summer Conditions

**Rogério Duarte [1], Maria da Glória Gomes [2,*], António Moret Rodrigues [2] and Fernando Pimentel [1]**

1 CINEA, Department of Mechanical Engineering, Instituto Politécnico de Setúbal, ESTSetúbal, Campus do IPS, Estefanilha, 2914-508 Setúbal, Portugal; rogerio.duarte@estsetubal.ips.pt (R.D.); fernando.pimentel@estsetubal.ips.pt (F.P.)
2 CERIS, Department of Civil Engineering, Architecture and Environment, Instituto Superior Técnico, Universidade de Lisboa, Av. Rovisco Pais, 1, 1049-001 Lisboa, Portugal; moret.rodrigues@tecnico.ulisboa.pt
* Correspondence: maria.gloria.gomes@tecnico.ulisboa.pt

**Abstract:** Earth–air heat exchangers (EAHX) use the soil thermal capacity to dampen the amplitude of outdoor air temperature oscillations. This effect can be used in hot and dry climates for room cooling, and depending on the EAHX design, this cooling can be achieved with very few resources other than those used during EAHX construction. This is an obvious advantage compared to the significant energy consumption and operational costs of refrigeration machines traditionally used in room cooling. Despite the large number of papers on EAHXs available in the scientific literature, very few deal with large-diameter EAHXs (with pipe diameters larger than 0.30 m), and even fewer present monitoring data gathered from a built and functional large-diameter EAHX. The present paper uses monitoring data and provides a detailed quantitative analysis of the performance of a large-diameter EAHX built for standalone cooling of an existing office building. The field monitoring was carried out during a characteristic hot and dry summer period of the south of Portugal. Results show that outdoor air to EAHX exit air temperature gradients reach 9 K and cooling capacities exceed 27 kW. Moreover, the studied EAHX is capable of standalone cooling for outdoor air temperatures up to 33 °C and meets more than 50% of the room design cooling demand for outdoor air temperatures as high as 37 °C. This evidences that large-diameter EAHXs have the potential to achieve significant reductions in $CO_2$ emissions and in energy consumption associated with building cooling in hot and dry climates.

**Keywords:** earth–air heat exchanger (EAHX); monitoring; load removal; room cooling; office building



**Citation:** Duarte, R.; Gomes, M.d.G.; Moret Rodrigues, A.; Pimentel, F. A Large-Diameter Earth–Air Heat Exchanger (EAHX) Built for Standalone Office Room Cooling: Monitoring Results for Hot and Dry Summer Conditions. *Appl. Sci.* **2023**, *13*, 12134. https://doi.org/10.3390/app132212134

Academic Editor: Weihua Cai

Received: 20 October 2023
Revised: 5 November 2023
Accepted: 6 November 2023
Published: 8 November 2023



## 1. Introduction

Building operation accounts for approximately one-third of the world's final energy consumption and also for approximately one-third of the total energy sector $CO_2$ emissions [1]. Electricity use in buildings keeps increasing, and with an average annual growth of 4% since 2000 [2], electricity demand for space cooling is rapidly gaining importance compared to the demand for lighting, equipments or hot water production. The growth in electricity demand for space cooling is linked to the increased use of refrigeration machines—air-conditioning—which, besides increasing consumption, also affects peak electricity demand as a result of the simultaneous operation of air conditioners at full capacity during hot days.

To meet the Net Zero Emissions by 2050 Scenario [3], the increase in electricity demand for space cooling needs to be stopped; technologies complementary or alternative to the prevailing refrigeration machines, allowing for a reduction in both electricity consumption and installed electric capacity for space cooling, should be researched and promoted. Earth–air heat exchangers (EAHX) is one such technology.

According to Santamouris in [4] and Ascione et al. [5], for the Mediterranean region, up to 100% of building cooling demand can be covered by EAHXs coupled with appropriate building passive cooling techniques. In general, cooling demand reductions of 30% to 60% are commonly associated with the use of EAHXs [6–8]. These results reveal the extent of the savings in electricity consumption for cooling that could be achieved from a broader use of EAHXs. This paper is concerned with the study of a specific type of EAHX: large-diameter EAHXs. Monitoring data from a large-diameter EAHX are used to assess standalone EAHX cooling (replacing a refrigeration machine) of an office building with hot and dry summer conditions.

Despite the large number of papers dealing with EAHXs available in the scientific literature [9], the vast majority concern EAHXs with pipe diameters not exceeding 0.30 m. Smaller pipe diameters are easier to handle, are less expensive and allow for increased heat transfer coefficients [5,7]. However, pipe diameter is only one among many parameters influencing heat transfer in EAHXs. Pipe length, pipe depth (below soil surface), pipe material, pipe layout and soil thermal properties are also crucial for EAHX performance and can compensate for the smaller heat transfer coefficients of large-diameter pipes; see [10]. Sensitivity studies by different authors conclude that the effect of pipe diameter changes in EAHX performance is lower than the effect of changes in pipe length, pipe depth (within a certain range) or airflow velocity [7,10,11]. Moreover, smaller pipe diameters are not free from disadvantages. For a given airflow rate, pressure losses increase significantly as diameter decreases [12], incrementing substantially fan installed capacity, fan electricity consumption and EAHX operational costs. Additionally, with increased airflow velocity, a reduction in temperature gradient between pipe inflow and outflow takes place [7], limiting EAHX use for standalone cooling. To avoid these disadvantages, especially when large ventilation rates are required—as in office building cooling—compact arrays of small diameter pipes are often used [10,13–16]. However, since compact layouts interrupt the diffusion of heat [10], thermal saturation of the soil in the immediate vicinity of the pipes takes place with the consequent reduction in heat exchange with the soil.

An aspect seldom mentioned in EAHX research is related to maintenance. EAHX and the building it serves share the same life expectancy, which can reach 50 years. National and international standards ensuring hygienic condition of ventilation systems (e.g., VDI 6022 [17]) mandate regular inspections for the detection and correction of biological hazards. Internal inspection of small-diameter pipes using robots is common, but correction of eventual problems (mostly caused by faults during construction and installation) is often difficult for buried pipes. Man-sized larger pipe diameters enabling access for inspection and correction of problems is, hence, a significant advantage [18]. Indeed, maintenance and other non-heat-transfer related aspects, such as availability of unimpeded soil to bury the pipes, commercial availability of materials, contractors' familiarity with EAHX construction techniques and costs, are paramount to EAHX sizing and introduce practical constraints to optimal heat transfer in EAHXs. Larger-diameter pipes imply larger investment costs (materials and excavation), not only because of the diameter increase but also for the larger pipe length and/or depth required to compensate the reduction in heat transfer; still, EAHX and building construction costs are seldom independent and, in the authors' experience, cost increments related to the use of larger pipe diameters can represent but a small fraction of the total building costs (of course, this relies heavily on the type of soil; indeed, Ascione et al. [5] mention a ten-fold or larger increase in excavation cost between sand, clay or gravel and hard rock soils). In this context, as important as costs is the ability to demonstrate the benefits/energy savings of EAHXs, and this depends on experimental evidence. Monitoring results for large-diameter EAHXs (>0.30 m) used in room cooling are rare. Research on heat transfer in large tunnels, as presented in Lui et al. [19], Xiangkui et al. [20] and Yang et al. [21], uses monitoring data and provides valuable insights into the hygrothermal behaviour of large-diameter EAHXs. However, large tunnel specifications and operating conditions are different from those of EAHXs used for building cooling. Studies using EAHXs as pure passive (no fans) cooling systems [22,23] or associating EAHXs with solar chimneys [24] also tend to use larger pipe diameters—required to minimize pressure losses—however, most of these studies present numerical rather than monitoring results. This paper addresses this gap in the research literature and uses monitoring data to assess the standalone cooling capacity of a large-diameter EAHX delivering a nominal 8000 $m^3/h$ flowrate of cooled air to an office building in a region with hot and dry summers.

The present paper is structured as follows. Section 2—Materials and Methods—describes the office building served by the EAHX, describes the cooling and ventilation system into which the EAHX is included, introduces the indices used to assess EAHX performance and details the monitoring protocol. Section 3—Results and Discussion—uses monitoring data to characterize the outdoor conditions and challenges posed to standalone EAHX cooling and assesses the large-diameter EAHX cooling performance and design. Section 4 presents the conclusions.

## 2. Materials and Methods

### *2.1. The Building Served by the EAHX: Location, Climate and Relevant Features*

The studied large-diameter EAHX serves an office building located in Beja district, Alentejo, in the south of Portugal. Figure 1 provides the geographic location of the building.

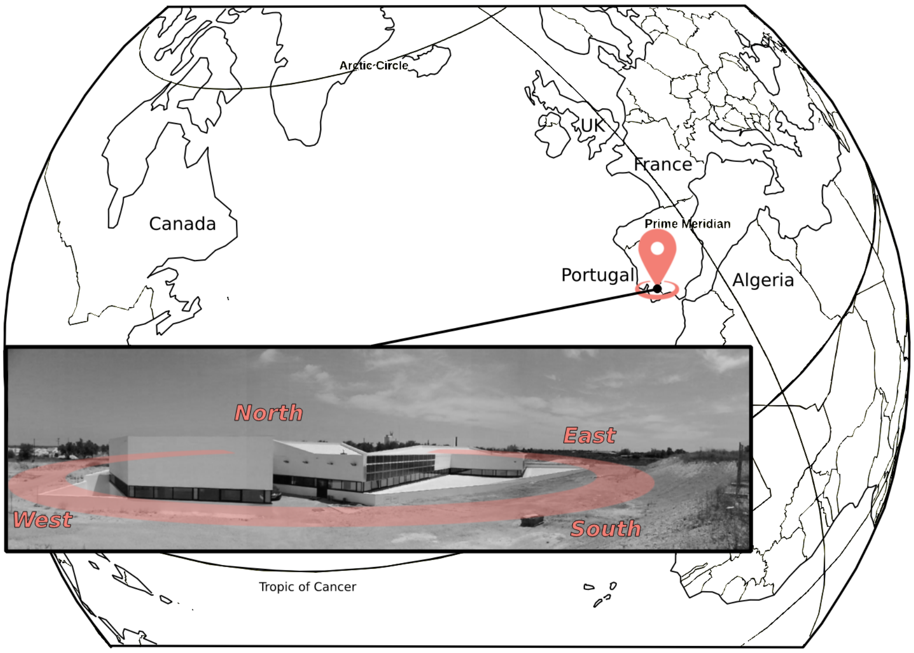


**Figure 1.** Location and a panoramic photograph of the west and south façades of the building being served by the EAHX.

Despite the proximity of Alentejo to the Atlantic Ocean, the presence of mountain ranges of Cercal and Grândola block the Atlantic influence, justifying climate varieties Csa (Mediterranean climate with hot and dry summer) and BSk (cold steppe climate of mid latitude) [25]. With large seasonal and diurnal temperature variations, these climate varieties are particularly suited to room cooling with EAHXs. The large seasonal outdoor temperature variation, with winter minimum temperatures lower than 0 °C and summer maximum temperatures reaching 40 °C, justify undisturbed soil temperatures of approximately 17 °C (at 3 m or larger depths), allowing, in the hot summer period, for significant temperature gradients between outdoor air and soil temperature and, therefore, significant cooling of outdoor air. The large diurnal outdoor temperature variations with nighttime minimum temperatures below soil temperature warrant the uninterrupted cycle of daily heating and cooling of the soil surrounding the EAHX pipes, preventing (or reducing) soil thermal saturation, and in this way, warranting the daily regeneration of the EAHX cooling capacity.

Figure 1 also includes a panoramic photograph of the building's west and south façades in the final construction stage. The building is one storey high and is developed along the west–east axis. It was designed with NZEB considerations in mind, which justified, besides the adoption of the EAHX for room cooling, partially buried exterior walls and photovoltaic panels on the south façade. These latter characteristics are visible in the panoramic photograph, namely, the buried walls below the windowsill and the photovoltaic panels extending from the lintel to ceiling height (the photograph depicts the initial stage of photovoltaic panels installation; once completed, photovoltaic panels covered the whole south façade). The EAHX, air handling unit (AHU) and distribution piping, being buried (in the south direction), are not visible.

Table 1 highlights building characteristics relevant to the study of the built EAHX.

**Table 1.** Building characteristics relevant to the study of the built EAHX.

| | |
|---|---|
| **Architectural** | |
| Layout | **(a)** A laboratory located at the west with larger ceiling height takes approximately 40% of the total building floor area. The remaining area—office area—with lower ceiling height extends towards the east, holding a technical room supporting the laboratory, research and administrative offices, a large meeting/training room, a reception, a restroom, WC and corridors connecting these spaces. Technical room, reception, and corridors lie on the north side of the building whilst offices and meeting room lie on the south side. The building is characterized by a small window-to-wall ratio. |
| Floor area | **(b)** Laboratory: 300 $m^2$; Office area: 450 $m^2$. |
| Room height | **(c)** For the cooled office area: 3 m. |
| **Envelope (thermal characteristics)** | |
| Exterior walls | **(d)** From the outside to the inside: mortar (30 mm), extruded polystyrene insulation board (XPS, 80 mm), cement bricks (300 mm), mortar (30 mm). U-value of 0.36 W/(m K) [26]. |
| Pavement floor | **(e)** From the outside to the inside: concrete slab (200 mm), XPS insulation board (60 mm), screed (60 mm). U-value of 0.39 W/(m K) [27]. |
| Ceiling | **(f)** Occupied spaces separated from an inverted roof (insulated on the outside with 60 mm XPS) by a false ceiling comprising (from the outside to the inside): mineral wool (60 mm), gypsum board (12 mm). U-value of 0.6 W/(m K) [26]. |
| Windows and shading | **(g)** Double-glazed (6 mm + 12 mm + 8 mm) window with solar control (solar factor, 0.33; U-value of 1.4 W/(m K)) and aluminium frame with thermal break. In the summer, slightly recessed windows and photovoltaic panels placed over the windows on the south façade block out direct solar radiation. |
| **Occupancy** | |
| | **(h)** Low occupancy density (lower than 0.03 person/$m^2$), weekdays from 8 to 18 h. |

Considering the low occupancy density, the envelope insulation, the large useful thermal mass and the larger indoor temperatures "allowed" by adaptive comfort principles—see item (m) of Table 2 in Section 2.2—20 W/$m^2$ (a specific load, defined per square meter of cooled floor area) was the *design* (or peak) cooling demand determined for the cooled rooms. Despite this low value—for an office building and hot summer climate—, to the design of an EAHX for standalone office room cooling it represents a challenging requirement.

## 2.2. The Cooling and Ventilation System

The installed cooling and ventilation system consists of the EAHX, an AHU, the distribution piping buried between the AHU and the building and the diffusion of air and temperature control in the cooled rooms. An outline schematic of this system is presented in Figure 2.

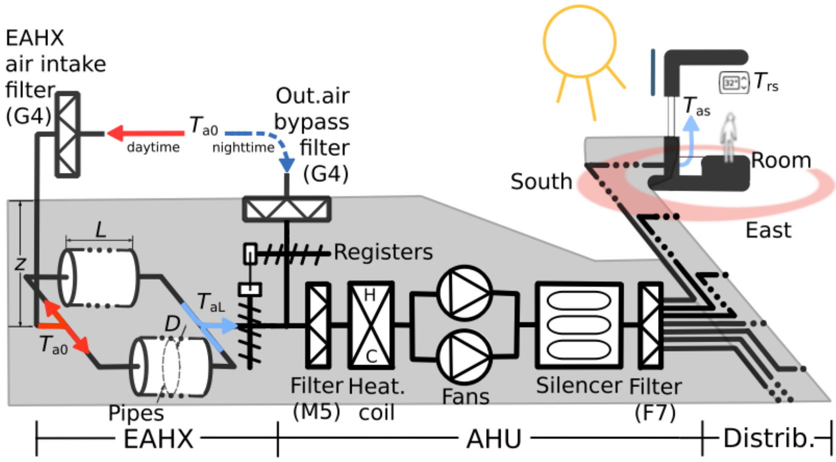


**Figure 2.** Outline schematic of the cooling and ventilation system.

Figure 2 represents (from left to right) the EAHX, the AHU and the distribution piping. Supply of cooled air to a room along the exterior wall at floor level, as well as a room temperature controller, are also depicted. Detailed specifications of the cooling and ventilation system are provided in Table 2.

**Table 2.** Cooling and ventilation system specifications.

| | |
|---|---|
| **EAHX** | |
| Pipes | **(a)** The EAHX consists of two pipes (concrete) with 1 m diameter placed 4 m apart (distance between axes), 70 m long, buried 5.5 m deep (average depth, since pipes are sloped towards the air intake for water drainage). Water-resistant coatings prevent the transfer of water across the pipes towards/from the soil. The pipes' inner surface coating has fungicidal and bactericidal properties to prevent the growth of mold and bacteria. |
| Air intake | **(b)** Outdoor air is admitted into the buried pipes at a technical space built above ground. A G4 filter [28] installed in this technical space prevents the intake of spores, pollen and coarse dust. |
| Vegetative cover | **(c)** To reduce soil surface temperature (during the summer period), species found in tallgrass prairies (e.g., Lolium perenne, Festuca arundinacea, Poa pratensis, Festuca rubra) were planted covering the ground above the EAHX. |
| Pressure loss | **(d)** Due to the large pipe diameter, pressure loss in the EAHX is related to the air intake filter, which, with its large surface and low face velocity, has negligible pressure loss compared to that in the AHU and in the distribution piping. |
| **AHU** | |
| Generic description | **(e)** In the direction of the airflow, the EAHX consists of a mixing chamber fitted with registers to allow for EAHX bypass with outdoor air (not used in this study), an M5 filter [28], a heating coil (not used in this study), two fans, a silencer and, prior to the air distribution to the rooms, a final F7 filter [28] for fine dust particles (1∼10 µm), preventing the distribution into rooms of bacteria and germs carried on host particles. As for the EAHX air intake, a coarse G4 filter is used at the bypass outdoor air intake. AHU dimensions were intentionally oversized to reduce pressure loss. |
| Fans | **(f)** To supply a nominal flowrate of 8000 $m^3/h$ of air to the rooms, a redundant set of two electrically commutated plug fans (IE5) with 3.6 kW rated power each are used. |
| Pressure loss | **(g)** Design pressure loss in the AHU is 325 Pa. |
| **Distribution piping** | |
| Generic description | **(h)** Cooled air is distributed to the rooms using high-density polyethylene (HDPE) corrugated pipes with varying diameters (<0.40 m) laid along the south façade of the building. Pipes run inside a rectangular pathway, buried 3.0 to 1.5 m deep, made of cement (bottom) and cement blocks (side walls). This pathway is (inside) insulated with XPS (60 mm), limiting heat loss to the soil (through the sides and bottom). |
| Pressure loss | **(i)** Design pressure loss in the distribution piping is 375 Pa. |

**Table 2.** *Cont.*

| **Diffusion of air and temperature control in the cooled rooms** | |
|---|---|
| Generic ventilation strategy | **(j)** A 100% fresh air system. Forced (cooled) air is supplied to the rooms at the south façade and at the reception through linear air diffusers placed along the exterior wall at floor level. Air flows to corridors and from there to the outside, exiting the building behind the south façade photovoltaic panels. |
| Pressure loss | **(k)** Linear air diffusers' specification is such that pressure loss associated with the introduction of supply air in the rooms is negligible compared to that in the AHU and in the distribution piping. |
| Temperature control | **(l)** Temperature control in the cooled rooms is achieved by varying the air-change rate. This control is limited by outdoor air conditions and by heat transfer with the soil. The control law depends (for hot and dry conditions) on room air and room setpoint temperatures, on EAHX exit air temperature, and on outdoor air temperature. To compensate for the system lower room-to-supply-air temperature gradients, large air-change rates are allowed [10,18]. Special attention is given to the specification of linear air diffusers so that larger airflow velocities in the room do not cause local discomfort with draught. |
| Temperature setpoint | **(m)** Adaptive comfort principles are assumed allowing free-floating room temperatures correlated to outdoor air temperatures. In other words, room setpoint temperature is allowed to vary and may be larger than setpoints typically associated with refrigeration machine cooling (>27 °C). |
| Nighttime ventilation | **(n)** Nighttime forced ventilation with cold outdoor air is used in two ways. Firstly, in combination with heavyweight building construction materials (insulated on the outside), making use of the walls' and floor's large thermal lag times to decrease room peak cooling requirements and decrease operative room temperatures. Secondly, in combination with the soil covering the insulated rectangular pathway for the distribution piping, allowing the use of the soil thermal mass to increase thermal lag times, contributing to additional daytime cooling of EAHX exit air. |

A photograph of the EAHX during construction is presented in Figure 3. This photograph shows a trench, the EAHX air intake at the start of the trench and two parallel pipes leaving this air intake towards the air handling unit (the latter not visible). Sketches of the air intake technical space built above ground and of the airflow pathway in the pipes were superimposed onto the photograph.

### 2.3. EAHX Performance Assessement

Figure 4 sketches, for a typical summer day, outdoor air temperature ($T_{a0}$) as it enters the EAHX and EAHX exit air temperature ($T_{aL}$) as it leaves the EAHX. It also represents room setpoint temperature limits—$T_{rs}^{U}$ and $T_{rs}^{L}$, with superscripts "U" and "L" standing for upper limit and lower limit, respectively, between which thermal comfort in a room is judged appropriate.

Figure 4 shows that in the morning, with office rooms already being used, outdoor air temperatures ($T_{a0}$) are lower than the room upper setpoint temperature ($T_{rs}^{U}$), allowing for free cooling with outdoor air. In the afternoon, since outdoor air temperatures exceed the upper setpoint temperature, the cooling of outdoor air becomes necessary. During nighttime, outdoor air temperatures lie below the lower setpoint temperature ($T_{rs}^{U}$); still, since the office building is unoccupied, there is no need for heating (actually, as described in item (n) of Table 2, during nighttime, forced ventilation with cold outdoor air can be used in combination with heavyweight building construction elements and with the soil in the buried pathway between AHU and rooms to assist daytime EAHX cooling).

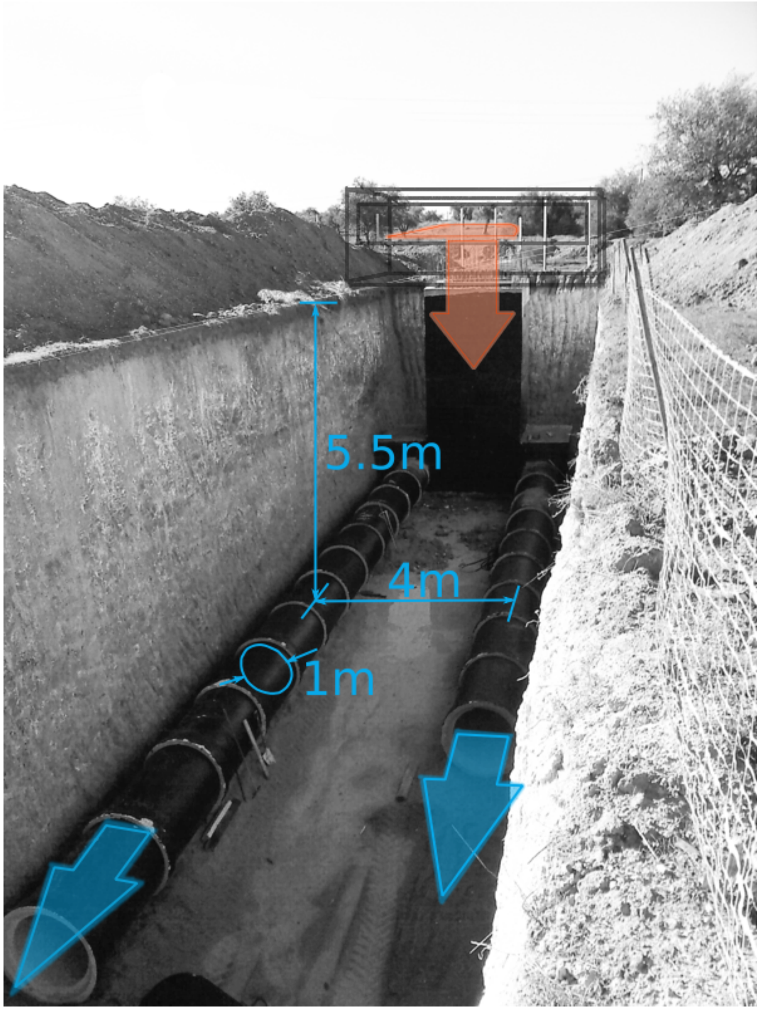


**Figure 3.** Photograph of the EAHX while the buried pipes were being installed at an average depth of 5.5 m below soil surface.

The pattern of the EAHX exit air temperature is similar to the outside air temperature but dampened and slightly forward shifted in time. The extent of the dampening and of the forward shifting determines EAHX cooling performance.

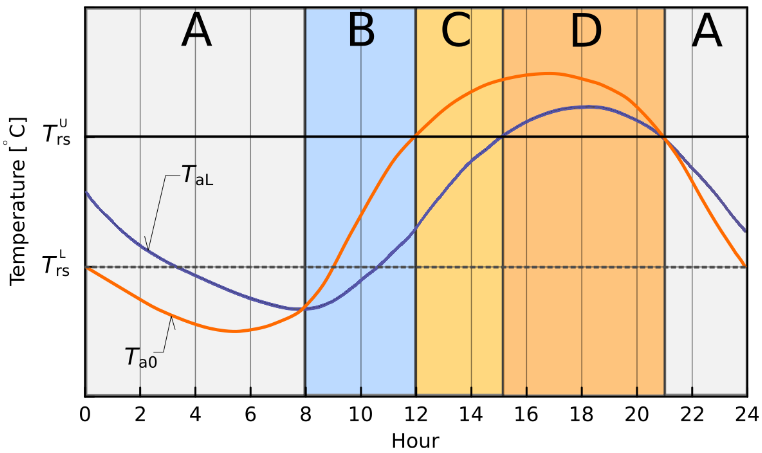


**Figure 4.** Sketch of outdoor air (entering the EAHX) and EAHX exit air temperatures for a typical summer day. Room upper and lower setpoint temperatures delimiting office room thermal comfort also represented.

To assess the cooling performance of an EAHX, two main indices are used (monitoring data confirm negligible latent heat exchanges in the EAHX during the dry summer period; further details provided in Section 3.1):

- EAHX outdoor air load removal,

$$\dot{Q}_{\mathrm{oa}}^{\mathrm{EAHX}} = \dot{m}_{\mathrm{a}} c_{\mathrm{a}} \Delta T_{\mathrm{aL,a0}}; \tag{1}$$

- EAHX room load removal,

$$\dot{Q}_{\mathrm{r}}^{\mathrm{EAHX}} = \dot{m}_{\mathrm{a}} c_{\mathrm{a}} \Delta T_{\mathrm{aL,rs}}; \tag{2}$$

where the gradients $\Delta T_{\mathrm{aL,a0}}$ and $\Delta T_{\mathrm{aL,rs}}$ are defined as

$$\Delta T_{\mathrm{aL,a0}} = \begin{cases} T_{\mathrm{aL}} - T_{\mathrm{a0}} & \text{if } T_{\mathrm{aL}} < T_{\mathrm{a0}}; \\ 0 & \text{otherwise}; \end{cases} \tag{3}$$

and

$$\Delta T_{\mathrm{aL,rs}} = \begin{cases} T_{\mathrm{aL}} - T_{\mathrm{rs}}^{\mathrm{U}} & \text{if } T_{\mathrm{aL}} < T_{\mathrm{rs}}^{\mathrm{U}}; \\ 0 & \text{otherwise}\,. \end{cases} \tag{4}$$

EAHX outdoor air load removal is a useful performance metric to assess EAHX "total" cooling capacity. However, when studying standalone EAHX cooling, EAHX room load removal is a much more appropriate performance metric, as it assesses EAHX "effective" *room* cooling capacity. Divided by the (cooled) room floor area,

$$\dot{q}_{\mathrm{r}}^{\mathrm{EAHX}} = \frac{\dot{Q}_{\mathrm{r}}^{\mathrm{EAHX}}}{A_{\mathrm{r}}}, \tag{5}$$

with units $\mathrm{W/m^2}$, the specific EAHX room load removal allows for a straightforward comparison to the room *design* cooling demand, a fundamental parameter in HVAC design (in general, $\dot{q}_{\mathrm{j}}^{\mathrm{EAHX}} = \dot{Q}_{\mathrm{j}}^{\mathrm{EAHX}}/A_{\mathrm{r}}$, with $j \in \{\mathrm{ao,r}\}$).

Given the outdoor air and EAHX exit air temperatures' dynamic nature, to assist the detailed analysis of the EAHX performance indices, regions A, B, C and D—see Figure 4—were defined. These regions are characterized as follows:

- **Region A**: Nighttime (from evening to the start of the working day) with outdoor air temperature lower than EAHX exit air temperature, $T_{\mathrm{a0}} < T_{\mathrm{aL}}$.

  In this region, the EAHX heats the outdoor air, operating, therefore, in heating mode. Since this paper discusses cooling performance, Region A is excluded from the analysis.
- **Region B**: From the start of the working day to noon with EAHX exit air temperature lower than outdoor air temperature and both of these lower than the upper room setpoint temperature, $T_{\mathrm{aL}} < T_{\mathrm{a0}} < T_{\mathrm{rs}}^{\mathrm{U}}$.

  In this region, the EAHX cools the outdoor air, operating, therefore, in cooling mode. Since the outdoor air temperature is lower than the room upper setpoint temperature, EAHX room load removal has two components,

$$\dot{Q}_{\mathrm{r}}^{\mathrm{EAHX}} = \dot{Q}_{\mathrm{oa}}^{\mathrm{EAHX}} + \dot{Q}_{\mathrm{r}}^{\mathrm{OA}} = \dot{m}_{\mathrm{a}} c_{\mathrm{a}} \Delta T_{\mathrm{aL,a0}} + \dot{m}_{\mathrm{a}} c_{\mathrm{a}} \Delta T_{\mathrm{a0,rs}}, \tag{6}$$

  namely, the EAHX outdoor air load removal component, $\dot{Q}_{\mathrm{oa}}^{\mathrm{EAHX}}$; and the outdoor air room free-cooling component, $\dot{Q}_{\mathrm{r}}^{\mathrm{OA}}$ (actually, this latter component is independent of the EAHX; however, because the flow of outdoor air in large-diameter EAHXs has negligible added fan cost—negligible pressure losses—, $\dot{Q}_{\mathrm{r}}^{\mathrm{OA}}$ is absorbed into $\dot{Q}_{\mathrm{r}}^{\mathrm{EAHX}}$). In Equation (6), the outdoor air to room upper setpoint temperature gradient, $\Delta T_{\mathrm{a0,rs}}$, is defined as,

$$\Delta T_{\mathrm{a0,rs}} = \begin{cases} T_{\mathrm{a0}} - T_{\mathrm{rs}}^{\mathrm{U}} & \text{if } T_{\mathrm{a0}} < T_{\mathrm{rs}}^{\mathrm{U}}; \\ 0 & \text{otherwise}. \end{cases} \tag{7}$$

In region B, due to outdoor air free cooling, the following inequation applies: $\dot{Q}_{\mathrm{r}}^{\mathrm{EAHX}} \geq \dot{Q}_{\mathrm{oa}}^{\mathrm{EAHX}}$.

- **Region C**: Start of the afternoon with EAHX exit air temperature lower than the room upper setpoint temperature and both of these lower than outdoor air temperature, $T_{\mathrm{aL}} < T_{\mathrm{rs}}^{\mathrm{U}} < T_{\mathrm{a0}}$.

  In this region, outdoor air makes no contribution to room cooling; still, it is customary to distinguish two components in the EAHX outdoor air load removal,

$$\dot{Q}_{\mathrm{oa}}^{\mathrm{EAHX}} = \dot{Q}_{\mathrm{r}}^{\mathrm{EAHX}} + \dot{Q}_{\mathrm{n}}^{\mathrm{EAHX}} = \dot{m}_{\mathrm{a}} c_{\mathrm{a}} \Delta T_{\mathrm{aL,rs}} + \dot{m}_{\mathrm{a}} c_{\mathrm{a}} \Delta T_{\mathrm{rs,a0}}, \tag{8}$$

  namely, the EAHX room load removal component, $\dot{Q}_{\mathrm{r}}^{\mathrm{EAHX}}$, and a component for the EAHX outdoor air load removal to the "neutral" state, $\dot{Q}_{\mathrm{n}}^{\mathrm{EAHX}}$, with

$$\Delta T_{\mathrm{rs,a0}} = \begin{cases} T_{\mathrm{rs}}^{\mathrm{U}} - T_{\mathrm{a0}} & \text{if } T_{\mathrm{rs}}^{\mathrm{U}} < T_{\mathrm{a0}}; \\ 0 & \text{otherwise}; \end{cases} \tag{9}$$

  being the temperature gradient that brings outdoor air to the room upper setpoint temperature, i.e., the condition for which outdoor air neither heats nor cools the room ("neutral" state).

  In region C, the following inequation applies: $\dot{Q}_{\mathrm{r}}^{\mathrm{EAHX}} \leq \dot{Q}_{\mathrm{oa}}^{\mathrm{EAHX}}$.

- **Region D**: During the afternoon, with room upper setpoint temperature lower than EAHX exit air temperature and both of these lower than outdoor air temperature, $T_{\mathrm{rs}}^{\mathrm{U}} < T_{\mathrm{aL}} < T_{\mathrm{a0}}$.

  In this region, since EAHX exit air temperature exceeds the room upper setpoint, the EAHX is incapable of removing room loads, $\dot{Q}_{\mathrm{r}}^{\mathrm{EAHX}} = 0$. The EAHX operates for outdoor air load removal only.

The analysis presented for the distinct regions—A, B, C and D—highlights the following conclusions:

- In region B, the EAHX complements free cooling with outdoor air, increasing room load removal.
- In region C, the EAHX replaces free cooling with outdoor air, increasing the duration of room load removal.
- A prime sizing requirement for standalone EAHX cooling is to avoid region D, i.e., for cooling design conditions, inequations $T_{\mathrm{aL}} < T_{\mathrm{a0}}$ and $T_{\mathrm{aL}} < T_{\mathrm{rs}}^{\mathrm{U}}$ should stand.

A final aspect relevant for standalone EAHX cooling performance is the definition of room upper setpoint temperature. When room cooling relies on refrigeration machines (including the case of EAHX designed solely for outdoor air precooling with a downwind refrigeration machine), "close control" of indoor air temperatures is possible; hence, a constant room setpoint is defined for the whole summer period. With standalone EAHX cooling, constant indoor air temperature can not be guaranteed. Indeed, standalone EAHX cooling resembles much more closely natural ventilation with window opening, with room temperature varying according to outdoor conditions. For naturally ventilated rooms, standard EN 15251:2007 [29] specifies free-floating room setpoint temperatures in accordance with adaptive comfort principles [30–32]. Given the resemblance to natural ventilation, previous researchers applied standard EN 15251:2007 and the adaptive comfort viewpoint to the study of EAHX [5,33]. This viewpoint is also used in this paper with free-floating room upper (U) setpoint temperatures defined as,

$$\begin{cases} T^{\mathrm{U}}_{\mathrm{rsIII}} = 0.33\theta_{\mathrm{rm}} + 18.8 + 4 & \Leftarrow \text{Category III;} \\ T^{\mathrm{U}}_{\mathrm{rsI}} = 0.33\theta_{\mathrm{rm}} + 18.8 + 2 & \Leftarrow \text{Category I;} \end{cases} \tag{10}$$

free-floating room lower (L) setpoint temperatures defined as,

$$\begin{cases} T^{\mathrm{L}}_{\mathrm{rsI}} = 0.33\theta_{\mathrm{rm}} + 18.8 - 2 & \Leftarrow \text{Category I;} \\ T^{\mathrm{L}}_{\mathrm{rsIII}} = 0.33\theta_{\mathrm{rm}} + 18.8 - 4 & \Leftarrow \text{Category III;} \end{cases} \tag{11}$$

and with subscripts III and I denoting acceptable and high comfort expectancy levels, respectively [29].

Equations (10) and (11) resort to the definition of running mean outdoor temperature, $\theta_{\mathrm{rm}}$, determined from [29]

$$\theta_{\mathrm{rm}} = (1-\beta)\left(\theta_{\text{ed-1}} + \beta\theta_{\text{ed-2}} + \beta^2\theta_{\text{ed-3+}\ldots}\right), \tag{12}$$

where

$\beta$ is a constant between 0 and 1 (0.8 is used in this study);
$\theta_{\text{ed-1}}$ is the daily mean external temperature for the previous day;
$\theta_{\text{ed-2}}$ is the daily mean external temperature for the day before, and so on.

### 2.4. Monitoring

Use of Equations (1) and (2) to assess EAHX performance requires monitoring of outdoor air temperature (to determine $T_{\mathrm{a0}}$, $\theta_{\mathrm{rm}}$ and $T^{\mathrm{U}}_{\mathrm{k}}$ with $k \in \{\mathrm{rsIII}, \mathrm{rsI}\}$); EAHX exit temperature ($T_{\mathrm{aL}}$); and airflow rate through the EAHX ($\dot{V}_{\mathrm{a}}$). To assess the relevance of latent heat exchanges in the EAHX, outdoor air relative humidity ($\phi_{\mathrm{a0}}$) was also monitored. To have an estimate of undisturbed soil temperature ($T_{\mathrm{s}\infty}$) at the EAHX depth, outdoor air temperature was monitored for a whole year and the average annual outdoor air temperature was determined; see [34].

A weather station [35] was installed at the EAHX location and started collecting outdoor data in late May. The built and functional EAHX was monitored during the summer period from 1 June to 30 September. During this period the EAHX operated in continuous mode, 24 h per day, 7 days per week, at the nominal airflow rate of 8000 m$^3$/h (4000 m$^3$/h per pipe). Table 3 characterizes the sensors used for data collection.

**Table 3.** Characteristics of the sensors used to monitor the performance of the built EAHX.

| **Outdoor Air (Vaisala Weather Station [35])** | |
|---|---|
| Out.air temp.sensor, $T_{\mathrm{a0}}$ | Duration: 1 year.<br>Log.frequency: 1 min.<br>Sensor location: Outdoor, ~1.5 m above ground in a unobstructed area.<br>Range: −53 to +60 °C.<br>Accuracy: ±0.3 °C (at 20 °C). |
| Out.air rel.hum.sensor, $\phi_{\mathrm{a0}}$ | Duration: 1 year.<br>Log.frequency: 1 min.<br>Sensor location: Outdoor, ~1.5 m above ground in a unobstructed area.<br>Range: 0 to 100%.<br>Accuracy: ±3% (from 0 to 90%); ±5% (from 90 to 100%). |

**Table 3.** *Cont.*

| **EAHX** | |
|---|---|
| Exit air temp. sensor, $T_{aL}$ (Onset datalogger [36]) | Duration: From 1 June to 30 September.<br>Log.frequency: 15 min.<br>Sensor location: AHU mixing chamber.<br>Range: −20 to +70 °C.<br>Accuracy: ±0.35 °C (from 0 to 50 °C). |
| Airflow rate, $\dot{V}_a$ (Fan controller module [37] measuring airflow rate from fan diff.pressure) | Duration: From 1 June to 30 September.<br>Log.frequency: 15 min.<br>Sensor location: AHU.<br>Range: 0 to 1000 Pa.<br>Accuracy: ±1.3% (max). |

Using sensors' characteristics in Table 3 and depicting measurement errors (assumed uncorrelated) as $\pm\delta(\cdot)$, it is possible to determine errors associated with the temperature gradient and heat transfer equations presented in Section 2.3. For the temperature gradient between air entering and exiting the EAHX, the error is constant and equal to

$$\pm\sqrt{\delta T_{aL}{}^2 + \delta T_{a0}{}^2} \simeq \pm 0.5\,^\circ\mathrm{C}\,. \tag{13}$$

For the heat transfer in the EAHX, assuming constant values of $c_a$ and $\rho_a$ (see Nomenclature) with $\delta\dot{V} = \pm 100$ m$^3$/h (=±0.0278 m$^3$/s), the measurement error associated with the nominal airflow rate (8000 m$^3$/h = 2.22 m$^3$/s), and using the maximum temperature gradient $\Delta T = 9$ K, with $\delta(\Delta T) = \pm 0.5$ °C, the maximum error is

$$\pm\rho_a c_a\sqrt{\Delta T^2 \delta\dot{V}^2 + \dot{V}^2\delta(\Delta T)^2} \simeq \pm 1400\ \mathrm{W}\,. \tag{14}$$

This maximum error applies to both $\dot{Q}^{\mathrm{EAHX}}_{\mathrm{oa}}$ and $\dot{Q}^{\mathrm{EAHX}}_{\mathrm{rIII}}$.

## 3. Results and Discussion

### *3.1. Outdoor Conditions and Challenges Facing Standalone EAHX Cooling*

Figure 5 presents outdoor air temperature ($T_{a0}$) data for the summer period between 1 June and 30 September.

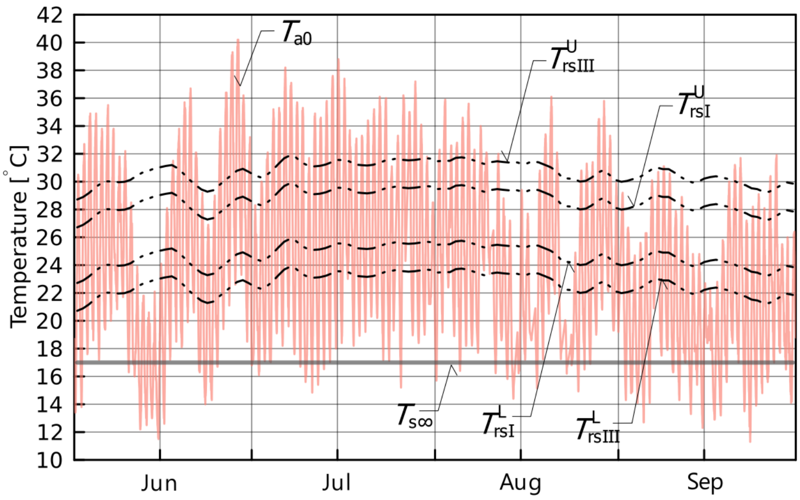


**Figure 5.** Timeseries of outdoor air temperature ($T_{a0}$, monitored data); upper and lower room setpoint temperatures ($T^{U}_{k}$ and $T^{L}_{k}$ with $k \in \{\mathrm{rsIII, rsI}\}$ determined from Equations (10) and (11) using monitoring data); estimate of undisturbed soil temperature ($T_{s\infty}$, determined from average annual outdoor air temperature data).

For the time period depicted in Figure 5, Table 4 presents monthly and summer (June–September) statistics of outdoor air temperature and of outdoor air relative humidity.

Table 4 shows that monthly median air temperatures exceeded 20 °C, reaching 26 °C in July. The outdoor air temperature range is largest in June, with maximum and minimum temperatures of 40 °C and 12 °C, respectively. The temperature range decreases in subsequent months, but maximum temperatures remain higher than 35 °C in July and August.

**Table 4.** Statistics for outdoor air temperature and relative humidity ($T_{a0}$ and $\phi_{a0}$, respectively). Obtained from summer monitoring data between 1 June and 30 September.

| | | **June** | **July** | **August** | **September** | **Summer (June–September)** |
|---|---|---|---|---|---|---|
| $T_{a0}$ [°C] | max. | 40.2 | 38.8 | 36.1 | 31.9 | 40.2 |
| | $Q_3$ | 29.3 | 31.1 | 28.2 | 24.7 | 28.3 |
| | median | 23.6 | 25.7 | 23.5 | 20.5 | 23.3 |
| | $Q_1$ | 19.3 | 21.0 | 19.3 | 17.5 | 19.1 |
| | min. | 11.5 | 14.9 | 14.4 | 11.3 | 11.3 |
| $\phi_{a0}$ [%] | max. | 93 | 88 | 90 | 92 | 93 |
| | $Q_3$ | 57 | 62 | 67 | 71 | 65 |
| | median | 41 | 44 | 51 | 54 | 47 |
| | $Q_1$ | 26 | 28 | 36 | 39 | 32 |
| | min. | 9 | 9 | 8 | 15 | 8 |

Table 4 also presents monthly and summer statistics of outdoor air relative humidity ($\phi_{a0}$). Confirming dry summer conditions, relative humidity interquartile range is defined between 32% and 65% with a median of 47% (June–September). An increase in monthly median relative humidity is observed from June (41%) to September (54%).

Using summer outdoor air temperature and relative humidity data, median and 95% percentile dew point temperatures of 11 and 16 °C (respectively) were determined [38]. Since these values are significantly lower than EAHX (pipes inner) surface temperatures (see Section 3.2), condensation in the EAHX has low likelihood, supporting the assessment of the EAHX cooling performance based on sensible heat exchanges (based on Equations (1) and (2)).

Figure 5 presents upper and lower room free-floating setpoint temperatures obtained from Equations (10) and (11) using monitoring data to derive the running mean outdoor temperature (Equation (12)). In spite of the large outdoor temperature variations (with daily ranges exceeding 15 K), the room setpoint variance is small. Statistics for these setpoints are presented in Table 5.

**Table 5.** Upper and lower free-floating room setpoint temperatures (categories III and I). Obtained for summer monitoring data between 1 June and 30 September.

| | $T^{U}_{rsIII}$ [°C] | $T^{U}_{rsI}$ [°C] | $T^{L}_{rsI}$ [°C] | $T^{L}_{rsIII}$ [°C] |
|---|---|---|---|---|
| max. | 31.9 | 29.9 | 25.9 | 23.9 |
| median | 30.8 | 28.8 | 24.8 | 22.8 |
| min. | 28.7 | 26.7 | 22.7 | 20.7 |

Table 5 confirms small variance in setpoints along the summer period with differences between median and maximum setpoints of only 1 K and setpoint ranges not exceeding 3 K.

It is obvious from Figure 5 that outdoor air temperatures exceed room upper setpoint temperatures throughout the whole summer. Furthermore, outdoor air temperatures lower than the room lower setpoint temperatures are also common. When discussing Figure 4, in Section 2.3, outdoor air temperatures above and below comfort limits were associated with daytime and nighttime, respectively. Since office rooms are unoccupied during nighttime, it was concluded that room heating was unnecessary. Figure 6 presents violin- and box-plots for outdoor air temperatures measured at different hours of the day.

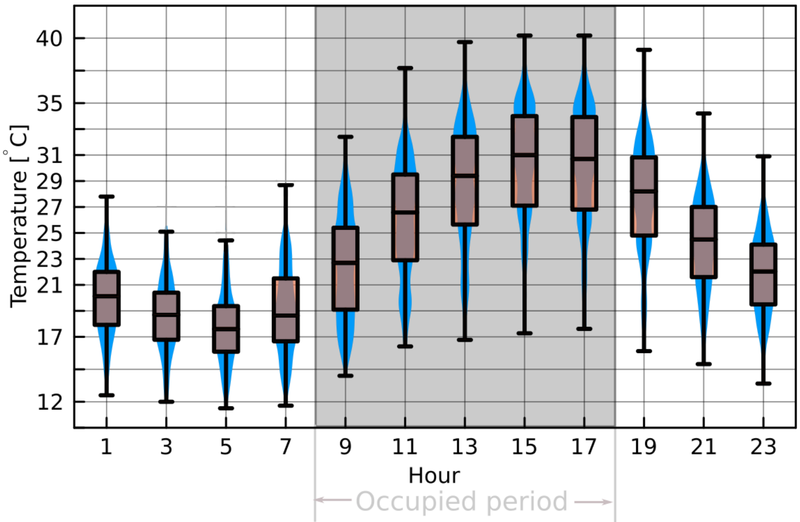


**Figure 6.** Hourly violin- and box-plots for outdoor air temperature. Obtained from summer monitoring data between 1 June and 30 September. Grey shading highlights room occupied period.

Figure 6 confirms that the lowest outdoor air temperatures, with median values lower than 19 °C, happen during nighttime, when office rooms are unoccupied. The significant reduction in median temperatures between daytime and nighttime also confirms that forced nighttime cooling with outdoor air can be used as a passive cooling technique, as described Table 2 item (n) and as mentioned in references [16,18,39].

Returning to the analysis of Figure 5, a line for the estimate of the undisturbed soil temperature ($T_{s\infty}$) at 5.5 m (the built EAHX burial depth) is also presented. Given the large temperature difference between this soil temperature estimate (17 °C) and Table 5 room upper setpoint medians (31 °C/29 °C for Category III/I), the feasibility of EAHX use for standalone room cooling is confirmed. Considering the temperature difference between these medians and the maximum outdoor air temperature (40 °C; see Table 4), it is concluded that for standalone EAHX cooling, the inflow to outflow temperature gradient ($\Delta T_{aL,a0}$) should be larger than 9 K/11 K (Category III/I). EAHX design, i.e., pipe length, depth, material and/or layout, should be such that the soil succeeds in reducing the outdoor air temperature in this order of magnitude, avoiding region D conditions.

### *3.2. EAHX Exit Air Temperature: Assessing EAHX Room Load Removal*

Figure 7 presents EAHX exit air temperature ($T_{aL}$) and EAHX airflow rate ($\dot{V}_a$) data for the summer period between 1 June and 30 September. To simplify the comparison to Figure 5, EAHX air exit temperatures are superimposed into a background of outdoor air temperature data and upper and lower room setpoint temperatures (categories III and I) are also depicted.

Figure 7 confirms that the ventilation rate was kept (approximately) constant at the nominal 8000 m$^3$/h rate. It also confirms a consistent reduction in air temperature amplitude between EAHX inflow (at outdoor temperature) and outflow (at EAHX exit temperature). Comparing time series of room upper setpoints with EAHX exit air temperatures shows that daily maximum exit temperatures seldom exceed Category I and never exceed Category III comfort expectancy levels. The built EAHX avoids, therefore, region D conditions for an acceptable comfort expectancy level (Category III) during the whole summer (June–September). For a higher comfort expectancy level (Category I), the built EAHX fails to deliver the required cooling with region D conditions in late June.

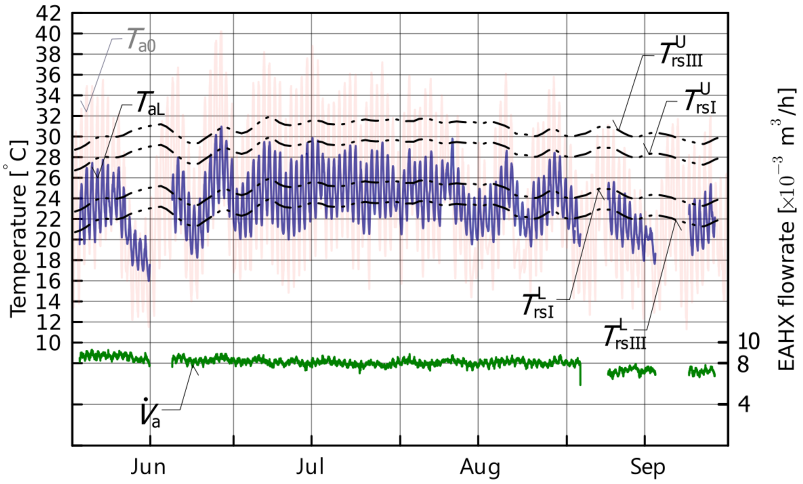


**Figure 7.** Timeseries of EAHX exit air temperature ($T_{aL}$, monitored data) and EAHX airflow rate ($\dot{V}_a$, monitored data). Upper and lower room setpoint temperatures and outdoor air temperature data also included.

Table 6 presents monthly and summer (Jun-Sep) statistics of EAHX exit air temperature ($T_{aL}$).

**Table 6.** Statistics for EAHX exit air temperature and for absolute value of EAHX exit air to outdoor air temperature gradient. Obtained from summer monitoring data between 1 June and 30 September.

| | | June | July | August | September | Summer (June–September) |
|---|---|---|---|---|---|---|
| $T_{aL}$ [°C] | max. | 31.0 | 29.9 | 29.8 | 25.6 | 31.0 |
| | $Q_3$ | 25.4 | 26.7 | 25.5 | 22.6 | 25.4 |
| | median | 23.0 | 24.4 | 23.7 | 21.1 | 23.3 |
| | $Q_1$ | 20.5 | 22.7 | 22.0 | 20.1 | 21.4 |
| | min. | 16.0 | 20 | 19.3 | 17.6 | 16.0 |
| $\lvert\Delta T_{aL,a0}\rvert$ $[K]$ [a] | max. | 10.9 | 9.1 | 9.2 | 7.1 | 10.9 |
| | $Q_3$ | 5.9 | 5.8 | 5.4 | 4.2 | 5.5 |
| | median | 3.7 | 4.2 | 3.9 | 2.5 | 3.7 |
| | $Q_1$ | 1.6 | 2.2 | 1.8 | 1.1 | 1.7 |
| | min. | ∼0 | ∼0 | ∼0 | ∼0 | ∼0 |

[a] Cooling only. Instants with $T_{aL} > T_{a0}$ excluded.

Comparing summer (June–September) statistics in Tables 4 and 6, the decrease in maximum temperature from 40 to 31°C and the increase in minimum temperature from 11 to 16 °C are observed; median outdoor air and EAHX exit air temperatures remain, however, equal (23.3 °C).

Table 6 includes statistics for the absolute value of temperature gradient $\Delta T_{aL,a0}$. Maximum and median summer (June–September) gradients are 11 and 4 K, respectively, and July is the month with the largest median gradient.

Figure 8 presents a scatter plot of temperature gradients $|\Delta T_{aL,a0}|$ used to obtain the statistics in Table 6 as a function of outdoor air temperature, $T_{a0}$.

From $|\Delta T_{aL,a0}|$ values in Figure 8, it is concluded that the EAHX cooling mode starts when the outdoor air temperature is approximately 19 °C (point 1, Figure 8). Since cooling is only possible when the EAHX (inner pipes) surface temperature is lower than the outdoor air temperature, 19 °C is an estimate of the lowest EAHX surface temperature for the cooling operating mode. Since null temperature gradients $|\Delta T_{aL,a0}|$ extend from 19 °C to 25 °C (from point 1 to point 2), this range is an estimate of the surface temperatures for which EAHX shifted between cooling and heating modes from 1 June and 30 September.

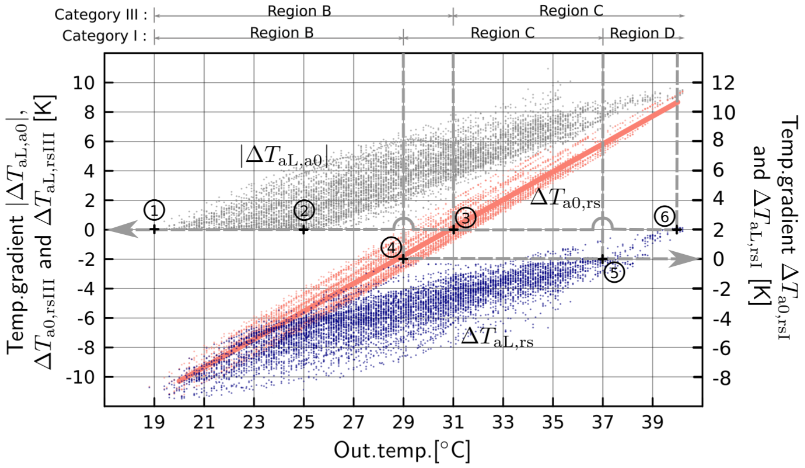


**Figure 8.** Various EAHX temperature gradients as a function of outdoor air temperature and trendline for $\Delta T_{\mathrm{a0,rs}}$. Obtained from monitored data (between 1 June and 30 September; cooling mode only, $T_{\mathrm{aL}} < T_{\mathrm{a0}}$; 8000 m$^3$/h nominal airflow rate). Left axis applies to $|\Delta T_{\mathrm{aL,a0}}|$, $\Delta T_{\mathrm{a0,rsIII}}$ and $\Delta T_{\mathrm{aL,rsIII}}$; right axis applies to $\Delta T_{\mathrm{a0,rsI}}$ and $\Delta T_{\mathrm{aL,rsI}}$.

Figure 8 also depicts temperature gradients $\Delta T_{\mathrm{a0,rs}}$ and $\Delta T_{\mathrm{aL,rs}}$. Directing the attention to these gradients, given that $|\Delta T_{\mathrm{aL,a0}}|$ is often approximately zero in the 19 °C to 25 °C range, gradients $\Delta T_{\mathrm{a0,rs}}$ and $\Delta T_{\mathrm{aL,rs}}$ are approximately equal, overlapping in Figure 8 for this range. As outside air temperature increases, $|\Delta T_{\mathrm{aL,a0}}|$ also increases; therefore, differences between $\Delta T_{\mathrm{a0,rs}}$ and $\Delta T_{\mathrm{aL,rs}}$ become visible: values of $\Delta T_{\mathrm{a0,rs}}$ are well approximated by a straight line, whilst values of $\Delta T_{\mathrm{aL,rs}}$ follow a curved line. For outdoor air temperatures of 31 °C and 29 °C—room upper setpoints for comfort categories III and I, respectively—temperature gradient $\Delta T_{\mathrm{a0,rs}}$ becomes 0 K (see point 3 and point 4; use left and right axes for $\Delta T_{\mathrm{a0,rsIII}}$ and $\Delta T_{\mathrm{a0,rsI}}$, respectively). When the outdoor air temperature increases to the maximum 40 °C, temperature gradient $|\Delta T_{\mathrm{aL,a0}}|$ increases to ∼9 K, precisely the difference between gradients $\Delta T_{\mathrm{a0,rs}}$ and $\Delta T_{\mathrm{aL,rs}}$.

With the help of gradients $\Delta T_{\mathrm{a0,rs}}$ and $\Delta T_{\mathrm{aL,rs}}$, regions B, C and D are delimited in Figure 8 for room comfort expectancy levels III and I. Figure 8 confirms, once more, that for Category III, the built EAHX avoids region D ($T_{\mathrm{aL}} < T^{\mathrm{U}}_{\mathrm{rsIII}}$). It provides further insight for the analysis of comfort Category I, showing that the EAHX is incapable of room cooling for outdoor air temperatures exceeding 37 °C (to the right of point 5, $T_{\mathrm{aL}} > T^{\mathrm{U}}_{\mathrm{rsI}}$). Note, however, that according to ASHRAE [38], for Beja (close to where the built EAHX is located), the 0.4%, 1.0% and 2.0% annual cooling dry-bulb design outdoor air temperatures are 37 °C, 35 °C and 33 °C, respectively. This means that for the Category I comfort level, the most demanding design criterion used in "traditional" (refrigeration machine) HVAC design—outdoor air temperature of 37 °C—equals the upper threshold for which the built EAHX is capable of room cooling. For the Category III comfort level, according to Figure 8, the upper threshold exceeds 40 °C (see point 6, with $T_{\mathrm{aL}} \leq T^{\mathrm{U}}_{\mathrm{rsIII}}$), allowing EAHX room load removal when outdoor air temperatures exceed the most demanding 0.4% design criterion.

### *3.3. EAHX Room Load Removal: Assessing Standalone EAHX Cooling and EAHX Design*

This section presents results for room comfort expectancy level III (Category III), which, according to the results of the previous section, allows for room cooling with the most demanding outdoor air design condition (37 °C), specified in ASHRAE [38].

From EAHX temperature gradients and EAHX airflow rate data, EAHX load removal was determined using Equations (1) and (2). Figure 9 highlights, for the room occupancy period between 8 and 18 h, hourly statistics of specific values (and absolute values) of EAHX room load removal $\dot{q}^{\mathrm{EAHX}}_{\mathrm{rIII}}$ ($\dot{Q}^{\mathrm{EAHX}}_{\mathrm{rIII}}$) and of EAHX outdoor air load removal, $\dot{q}^{\mathrm{EAHX}}_{\mathrm{oa}}$ ($\dot{Q}^{\mathrm{EAHX}}_{\mathrm{oa}}$).

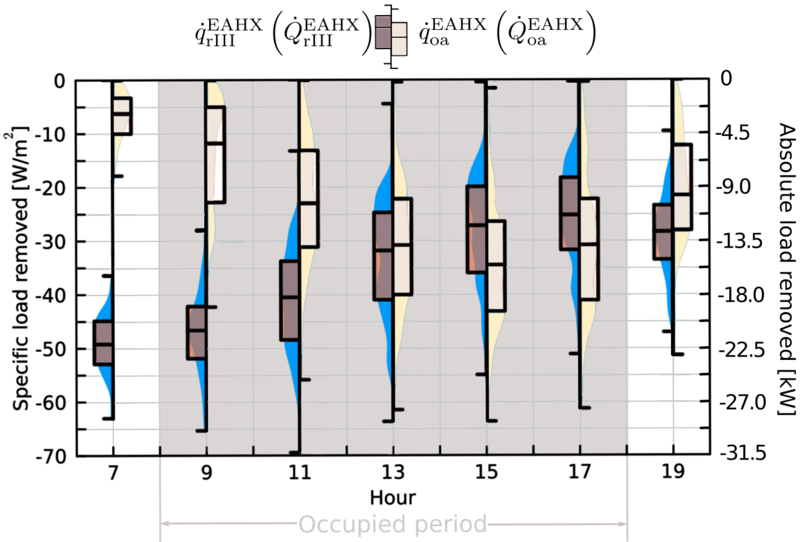


**Figure 9.** Hourly violin- and box-plots for specific (and absolute) EAHX room load removal—$\dot{q}_{\mathrm{rIII}}^{\mathrm{EAHX}}$ ($\dot{Q}_{\mathrm{rIII}}^{\mathrm{EAHX}}$)—and for specific (and absolute) EAHX outdoor air load removal—$\dot{q}_{\mathrm{oa}}^{\mathrm{EAHX}}$ ($\dot{Q}_{\mathrm{oa}}^{\mathrm{EAHX}}$). Obtained from monitored data (between 1 June and 30 September; cooling mode only, $T_{\mathrm{aL}} < T_{\mathrm{a0}}$; 8000 m$^3$/h nominal airflow rate; 450 m$^2$ of cooled floor area) considering Category III comfort expectation level. Grey shading highlights room occupied period. Left and right axis depict specific and absolute load removal, respectively.

As mentioned in Section 2.3 and confirmed in Figure 9, EAHX room load removal is larger during the morning, region B (the result of the added outdoor air free-cooling component, $\dot{Q}_{\mathrm{r}}^{\mathrm{OA}}$), whilst EAHX outdoor air load removal is larger during the afternoon, region C (the result of the added component $\dot{Q}_{\mathrm{n}}^{\mathrm{EAHX}}$). Figure 9 presents large absolute outdoor air load removal ($|\dot{Q}_{\mathrm{oa}}^{\mathrm{EAHX}}|$) during afternoons, with medians and maxima exceeding 13.5 kW and 27 kW, respectively. As regards specific room load removal ($|\dot{q}_{\mathrm{rIII}}^{\mathrm{EAHX}}|$), from Figure 9 it is concluded that median values of this performance index are always higher than 20 W/m$^2$, the room *design* (or peak) cooling demand (recall Section 2.1). However, during the afternoon, when summer outdoor conditions are more demanding and when the design outdoor air temperature typically applies [38], interquartile ranges for $|\dot{q}_{\mathrm{rIII}}^{\mathrm{EAHX}}|$ are very wide, extending from ∼0 W/m$^2$ ($Q_1$) to above 50 W/m$^2$ ($Q_3$). It is, hence, important to assess in more detail the actual EAHX room load removal for hot afternoons.

Using monitoring data, Figure 10 presents the following conditional probability distributions, $P\left(|\dot{q}_{\mathrm{rIII}}^{\mathrm{EAHX}}| \geq \dot{q}_{\mathrm{r}}^{\mathrm{BLDG}} | T_{\mathrm{a0}} = T\right)$ with $\dot{q}_{\mathrm{r}}^{\mathrm{BLDG}} \in \mathbb{R}$ and $T \in \{33\ ^{\circ}\mathrm{C}, 35\ ^{\circ}\mathrm{C}, 37\ ^{\circ}\mathrm{C}\}$, i.e., the probability that the EAHX delivers a specific (room) cooling capacity greater or equal to the specific room cooling demand, $\dot{q}_{\mathrm{r}}^{\mathrm{BLDG}}$, conditional to outdoor air temperature being equal to Beja's 2%, 1% or 0.4% design dry-bulb outdoor air temperatures [38].

Figure 10 shows that for Beja's 2% design dry-bulb outdoor air temperature ($T_{\mathrm{a0}} = 33\ ^{\circ}\mathrm{C}$), the probability that the EAHX meets the 20 W/m$^2$ room peak cooling demand is 84%. Therefore, considering this (less demanding) outdoor air temperature design criterion, standalone use of the built EAHX for office room cooling is accepted.

For the 1% design dry-bulb outdoor air temperature ($T_{\mathrm{a0}} = 35\ ^{\circ}\mathrm{C}$), the probability that the EAHX meets the 20 W/m$^2$ room peak cooling demand reduces to 45%, and for the most demanding 0.4% design criterion, this probability is less than 5%. For these moderate and more demanding criteria ($T_{\mathrm{a0}} \geq 35\ ^{\circ}\mathrm{C}$), it is concluded that standalone use of the built EAHX does not provide sufficient cooling and does not warrant room temperatures below the upper setpoint. Still, Figure 10 shows that the built EAHX delivers room cooling capacities of 10 W/m$^2$ with approximately 100% probability, and delivers room cooling capacities of 15 W/m$^2$ with 32% to ∼100% probabilities (from 0.4% to 2% design dry-bulb outdoor air temperatures). This means that despite being insufficient, a significant part of the room design cooling demand (at least more than 50%) is already provided by the built EAHX.

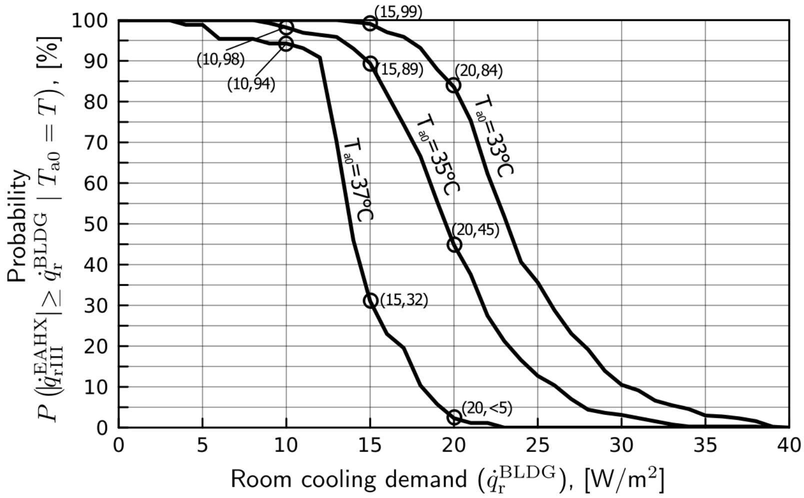


**Figure 10.** Probability that the EAHX specific (room) cooling capacity is greater or equal to a specific room cooling demand, $\dot{q}_{\mathrm{r}}^{\mathrm{BLDG}}$; conditional to outdoor air temperature being equal to $T$. Obtained from monitored data (between 1 June and 30 September; cooling mode only, $T_{\mathrm{aL}} < T_{\mathrm{a0}}$; 8000 m$^3$/h nominal airflow rate; 450 m$^2$ of cooled floor area) considering Category III comfort expectation level.

As regards the built EAHX standalone use, these results lead to the following conclusions:

(i) The built EAHX operates in standalone mode, delivering the required room *design* (or peak) cooling demand and providing acceptable comfort in the cooled rooms (Category III [29]), if outdoor air temperature does not exceed 33 °C (2% annual cooling design dry-bulb outdoor temperature [38]).

(ii) For outdoor air temperatures exceeding 33 °C, the built EAHX allows for room cooling during the whole summer; however, room load removal is insufficient to meet the room *design* cooling demand. If room comfort Category III is judged to be appropriate, the built EAHX provides, on its own, more than 50% of the room *design* cooling demand.

(iii) If high room comfort is expected (Category I [29]), the built EAHX ceases room cooling for outdoor temperatures exceeding 37 °C (the 0.4% annual cooling design dry-bulb outdoor temperature [38]).

To meet/deliver the additional room cooling demand necessary for cases (ii) and (iii) above, the following strategies could be implemented:

1. Alter the EAHX design; for example, increase pipe length, change pipe layout.
2. Complement EAHX room load removal with passive cooling techniques, e.g., forced nighttime ventilation and appropriate use of building thermal mass.

The first of the above strategies is useful for future EAHX design, not for the built one.

The second strategy is described in Zimmermann et al. [16] and several other authors [10,18], and is available with the researched cooling and ventilation system, as already mentioned in Table 2, item (n). The analysis of the performance of the hybrid EAHX-TM cooling and ventilation system (as classified by Soares et al. [39], with TM standing for building thermal mass), requiring the joint research of the built EAHX and the existing building/distribution piping, falls out of the scope of this paper. However, considering experimental results found in studies dealing with building nighttime ventilation [18,40,41], with significant (∼2 K) room peak temperature reductions and the significant decrease in refrigeration machine cooling need (up to 50% reduction [42]), the built hybrid EAHX-TM system should extend the range of outdoor air temperatures for which the room *design* cooling demand is met.

## 4. Conclusions

In this study, the thermal and energy performance of an existing large-diameter earth–air heat exchanger (EAHX) was evaluated as a strategy for standalone cooling of a small existing office building. The study used monitored data gathered during the summer period at the EAHX location, in Alentejo, a region in the south of Portugal characterized by hot and dry summer conditions. Outdoor and EAHX outflow air temperatures were registered and the loads removed in the EAHX were determined for the nominal airflow rate (8000 $m^3/h$). From the analysis of the experimental data and from the discussions presented, the paper's findings can be summarized as follows:

- The large temperature difference between the undisturbed soil temperature (~17 °C) and the room upper setpoint (~30 °C, considering adaptive comfort principles [29]) confirmed the feasibility of EAHX standalone cooling.
- Daily maximum EAHX outflow temperatures can be 9 K lower than the simultaneous outdoor air temperatures and results confirm that air exits the EAHX at temperatures that never exceed room upper setpoint for Category III, and that seldom exceed room upper setpoint for Category I comfort expectancy level [29].
- Median values of EAHX specific room load removal are larger than 20 $W/m^2$, the room *design* cooling demand; however, smaller EAHX room load removal occurs during the afternoon, precisely when the room cooling demand is higher.
- A detailed analysis of EAHX room load removal shows that the EAHX is capable of standalone cooling when outdoor temperatures do not exceed 33 °C. When this temperature is exceeded, standalone cooling would require changes in the EAHX design. Despite this limitation, the built EAHX is capable of delivering more than 50% of the required cooling (for Category III comfort expectancy) when outdoor temperatures are as high as 37 °C (the most demanding outdoor air temperature criterion used in "traditional" HVAC design [38]), and the combined use of the EAHX and passive cooling strategies (i.e., nighttime ventilation) should increase the cooling delivered, meeting the room *design* cooling demand.

Although this study has focused on monitoring data for a particular case, it showed that cooling with large-diameter EAHXs is feasible and that this technology fits the needs of buildings located in hot and dry climates. Used in standalone mode or in combination with building passive cooling techniques, large-diameter EAHXs extend the use of free cooling with outdoor air and can replace refrigeration machines for room cooling. These conclusions should remain valid for other projects with similar conditions; however, because construction costs vary significantly depending on the site and on the building design specifications, the decision to use a large-diameter EAHX for building cooling should be supported by a thorough investment analysis. Moreover, given the sharp difference to "traditional" (refrigeration machine) cooling, project promoters and key decision makers should be advised of the limitations associated with standalone EAHX cooling.

**Author Contributions:** Conceptualization, R.D., M.d.G.G. and A.M.R.; methodology, R.D., M.d.G.G. and A.M.R.; validation, R.D., A.M.R., M.d.G.G. and F.P.; formal analysis, R.D., A.M.R. and M.d.G.G.; investigation, R.D.; resources, R.D. and F.P.; data curation, R.D. and F.P.; writing—original draft preparation, R.D.; writing—review and editing, A.M.R., M.d.G.G. and F.P.; visualization, R.D.; project administration, M.d.G.G. and R.D. All authors have read and agreed to the published version of the manuscript.

**Funding:** The CERIS research unit (UIDB/04625/2020) to which the second and third authors belong is funded by the Portuguese Foundation for Science and Technology (FCT).

**Institutional Review Board Statement:** Not applicable.

**Informed Consent Statement:** Not applicable.

**Data Availability Statement:** Data are contained within the article.

**Acknowledgments:** The first author thanks Miguel Nuno Ferreira da Costa Santos, Eng.º, designer of the researched EAHX and of the office building cooling and ventilation system. Authors thank the team responsible for the management and maintenance of the studied office building for their support in the monitoring of the EAHX.

**Conflicts of Interest:** The authors declare no conflict of interest.

## Nomenclature

| | |
|---|---|
| $A$ | area, $m^2$ |
| $c$ | specific heat, J/(kg K), in this paper $c_a = 1020$ J/(kg K) |
| $D$ | diameter (EAHX pipe), m |
| $\dot{m}$ | mass-flow rate, kg/s (in this paper $\rho_a = 1.2$ kg/m$^3$) |
| $Q_1$ | first quartile, n.a. |
| $Q_3$ | third quartile, n.a. |
| $\dot{Q}$ | heat-transfer rate, W |
| $\dot{q}$ | specific heat-transfer rate, W/m$^2$ (of cooled floor area) |
| $T$ | temperature, °C |
| $\dot{V}$ | EAHX airflow rate, m$^3$/s |
| $z$ | depth (soil), m |
| $\beta$ | coefficient (taken as 0.8) used in Equation (12), none |
| $\delta(\cdot)$ | measurement error |
| $\Delta T$ | temperature gradient, K |
| $\theta$ | outdoor daily mean temperature, °C |
| $\phi$ | relative humidity, % |
| **Subscripts** | |
| I | denotes Category I comfort expectancy level |
| III | denotes Category III comfort expectancy level |
| a | denotes air |
| a0 | denotes air entering the EAHX |
| aL | denotes air exiting the EAHX |
| as | denotes air supplied to a room |
| oa | denotes outdoor air |
| r | denotes (cooled) room |
| rm | denotes running mean |
| rs | denotes room setpoint |
| s∞ | denotes undisturbed soil |
| **Superscipts and abbreviations** | |
| AHU | denotes air handling unit |
| BLDG | denotes building |
| EAHX | denotes earth–air heat exchanger |
| HVAC | denotes heating, ventilation and air-conditioning |
| L | denotes lower (setpoint) |
| NZEB | denotes nearly zero energy building |
| TM | denotes (building or soil) thermal mass |
| U | denotes upper (setpoint) |

## References


1. IEA. Buildings, IEA, Paris. License: CC BY 4.0. 2022. Available online: https://www.iea.org/reports/buildings (accessed on 2 May 2023).
2. IEA. Space Cooling, IEA, Paris. License: CC BY 4.0. 2022. Available online: https://www.iea.org/reports/space-cooling (accessed on 2 May 2023).
3. IEA. Global Energy and Climate Model: Documentation, IEA, Paris. License: CC BY 4.0. 2022. Available online: https://www.iea.org/reports/global-energy-and-climate-model (accessed on 2 May 2023).
4. Mihalakakou, G.; Santamouris, M.; Lewis, J.; Asimakopoulos, D. On the application of the energy balance equation to predict ground temperature profiles. *Sol. Energy* **1997**, *60*, 181–190. [CrossRef]
5. Ascione, F.; Bellia, L.; Minichiello, F. Earth-to-air exchanger for Italian climates. *Renew. Energy* **2011**, *36*, 2177–2188. [CrossRef]
6. Michalak, P. Hourly Simulation of an Earth-to-Air Heat Exchanger in a Low-Energy Residential Building. *Energies* **2022**, *15*, 1898. [CrossRef]
7. Lee, K.; Strand, R. The cooling and heating potential of an earth tube system in buildings. *Energy Build.* **2008**, *40*, 486–494. [CrossRef]
8. Al-Ajmi, F.; Loveday, D.; Hanby, V. The cooling potential of earth–air heat exchangers for domestic buildings in a desert climate. *Build. Environ.* **2006**, *41*, 235–244. [CrossRef]
9. Singh, B.; Asati, A.; Kumar, R. Evaluation of the Cooling Potential of Earth Air Heat Exchanger Using Concrete Pipes. *Int. J. Thermophys.* **2021**, *42*, 19. [CrossRef]
10. Hollmuller, P.; Lachal, B. Air-soil heat exchangers for heating and cooling of buildings: Design guidelines, potentials and constraints, system integration and global energy balance. *Appl. Energy* **2014**, *119*, 476–487. [CrossRef]
11. Kopecký, P. Hygro-Thermal Performance of Earth-to-Air Heat Exchangers: Numerical Model, Analytical and Experimental Validation, Measurements In-Situ, Design. Ph.D. Thesis, Czech Technical University in Prague, Prague, Czech Republic, 2008.
12. Recknagel, H.; Sprenger, E.; Schramek, E. *Taschenbuch für Heizung und Klimatechnik*; Oldenbourg Industrieverlag München: Munich, Germany, 2009.
13. Blümel, E.; Fink, C.; Reise, C. *Luftdurchströmte Erdreichwärmetauscher—Handbuch zur Plannung und Ausfürung von luftdurchströmten Erdreichwärmetauschern für Heiz- und Kühlanwendungen*; Technical Report; Erneuerbare Energie, AEE INTEC, Institut für Nachaltige Technologien: Gleisdorf, Österreich, 2001.
14. Huber, A.; Müller, C.; Berchtold, O.; Eggenberger, H. *Luftvorwärmung für Wärmepumpen in Erdregistern—Phase 1: Kosten, Nutzen, Analyse*; Technical Report; Huber Energietechnik und Trainingszentrum–Wärmepumpen, im Auftrag des Bundesamtes für Energie: Füllinsdorf, Switzerland, 1996.

15. Pfafferott, J. Evaluation of earth-to-air heat exchangers with a standardised method to calculate energy efficiency. *Energy Build.* **2013**, *35*, 971–983. [CrossRef]
16. Zimmermann, M. *Handbuch der Passiven Külung*; Technical Report; EMPA: Dübendorf, Switzerland, 1999.
17. *VDI 6022:2018*; Ventilation and Indoor-Air Quality: Hygiene Requirements for Ventilation and Air-Conditioning Systems and Units (VDI Ventilation Code of Practice). Verein Deutscher Ingenieur: Düsseldorf, Germany, 2018.
18. Barnard, N.; Jauzens, D.E. *IEA Annex 28 Subtask 2: Design Tools for Low Energy Cooling: Technology Selection and Early Design Guidance*; Technical Report; Building Research Establishment: Watford, UK, 2001.
19. Liu, X.; Xiao, Y.; Inthavong, K.; Tu, J. A fast and simple numerical model for a deeply buried underground tunnel in heating and cooling applications. *Appl. Therm. Eng.* **2014**, *62*, 545–552. [CrossRef]
20. Xiangkui, G.; Yongtong, Q.; Yimin, X. A numerical method for cooling and dehumidifying process of air flowing through a deeply buried underground tunnel with unsaturated condensation model. *Appl. Therm. Eng.* **2019**, *159*, 113891.
21. Yang, D.; Wei, H.; Wang, J.; He, M. Coupled heat and moisture transfer model to evaluate earth-to-air heat exchangers exposed to harmonically fluctuating thermal environments. *Int. J. Heat Mass Transf.* **2021**, *174*, 121293. [CrossRef]
22. Ferrucci, M.; Peron, F. Ancient Use of Natural Geothermal Resources: Analysis of Natural Cooling of 16th Century Villas in Costozza (Italy) as a Reference for Modern Buildings. *Sustainability* **2018**, *10*, 4340. [CrossRef]
23. Zhang, J.; Haghighat, F. Convective heat transfer prediction in large rectangular cross-sectional area Earth-to-Air Heat Exchangers. *Build. Environ.* **2009**, *44*, 1892–1898. [CrossRef]
24. Long, T.; Zheng, D.; Li, W.; Li, Y.; Lu, J.; Xie, L.; Huang, S. Numerical investigation of the working mechanisms of solar chimney coupled with earth-to-air heat exchanger (SCEAHE). *Sol. Energy* **2021**, *230*, 109–121. [CrossRef]
25. IPMA. Climate Normals—Köppen Climatic Classification. Available online: https://www.ipma.pt/en/oclima/normais.clima (accessed on 1 January 2023).
26. Pina dos Santos, C.; Matias, L. (Eds.) *ITE 50—Coefficients of Thermal Transmission for Building Envelope Elements*; LNEC: Lisboa, Portugal, 2010. (In Portuguese)
27. *EN 13370:2017*; Thermal Performance of Buildings—Heat Transfer via the Ground—Calculation Methods. European Committee for Standardization: Brussels, Belgium, 2017.
28. *EN 779:2012*; Particulate Air Filters for General Ventilation—Determination of the Filtration Performance. European Committee for Standardization: Brussels, Belgium, 2012.
29. *EN 15251:2007*; Indoor Environmental Input Parameters for Design and Assessment of Energy Performance of Buildings Addressing Indoor Air Quality, Thermal Environment, Lighting and Acoustics. European Committee for Standardization: Brussels, Belgium, 2007; Currently EN 16798-1:2019.
30. Nicol, J.; Humphreys, M. Adaptive thermal comfort and sustainable thermal standards for buildings. *Energy Build.* **2002**, *34*, 563–572. [CrossRef]
31. de Dear, R.J.; Brager, G.S. Thermal comfort in naturally ventilated buildings: Revisions to ASHRAE Standard 55. *Energy Build.* **2002**, *34*, 549–561. [CrossRef]
32. Raja, I.A.; Nicol, J.; McCartney, K.J.; Humphreys, M.A. Thermal comfort: Use of controls in naturally ventilated buildings. *Energy Build.* **2001**, *33*, 235–244. [CrossRef]
33. Maerefat, M.; Haghighi, A. Passive cooling of buildings by using integrated earth to air heat exchanger and solar chimney. *Renew. Energy* **2010**, *35*, 2316–2324. [CrossRef]
34. Givoni, B.; Katz, L. Earth temperatures and underground buildings. *Energy Build.* **1985**, *8*, 15–25. [CrossRef]
35. Vaisala. *Vaisala Weather Transmitter WXT520—User's Guide*; Vaisala Oyj: Vantaa, Finland, 2012. Available online: https://www.vaisala.com/sites/default/files/documents/M210906EN-C.pdf (accessed on 1 January 2023).
36. Onset. HOBO Datalogger Temp/RH/2 ext.Channels (U12-0011). Available online: https://www.onsetcomp.com/ (accessed on 1 January 2023).
37. Ziehl-Abegg. Ziehl-Abegg Sensor Control Module for Differential Pressure and Volume Flow Measurements. Available online: https://www.ziehl-abegg.com/en/products/control-modules#modelselection (accessed on 1 January 2023).
38. ASHRAE. *ASHRAE Handbook—Fundamentals*; ASHRAE: Peachtree Corners, GA, USA, 2005.
39. Soares, N.; Rosa, N.; Monteiro, H.; Costa, J. Advances in standalone and hybrid earth-air heat exchanger (EAHX) systems for buildings: A review. *Energy Build.* **2021**, *253*, 111532. [CrossRef]
40. Geros, V.; Santamouris, M.; Tsangrasoulis, A.; Guarracino, G. Experimental evaluation of night ventilation phenomena. *Energy Build.* **1999**, *29*, 141–154. [CrossRef]
41. Givoni, B. Effectiveness of mass and night ventilation in lowering the indoor daytime temperatures. Part I: 1993 experimental periods. *Energy Build.* **1998**, *28*, 25–32. [CrossRef]
42. Blondeau, P.; Spérandio, M.; Allard, F. Night ventilation for building cooling in summer. *Sol. Energy* **1997**, *61*, 327–335. [CrossRef]